THE JOURNAL OF BIOLOGICAL CHEMISTRY
Vol. 272, No. 31, Issue of August 1, pp. 19373–19382, 1997

Printed in U.S.A.

Electron Paramagnetic Resonance Studies of Succinate:Ubiquinone Oxidoreductase from *Paracoccus denitrificans*

EVIDENCE FOR A MAGNETIC INTERACTION BETWEEN THE 3Fe-4S CLUSTER AND CYTOCHROME *b**

(Received for publication, March 17, 1997, and in revised form, May 14, 1997)

A. Reginald Waldeck‡, Michael H. B. Stowell‡§, Hung Kay Lee‡, Shao-Ching Hung‡, Mikael Matsson¶, Lars Hederstedt¶, Brian A. C. Ackrell‖, and Sunney I. Chan‡**

From the ‡Arthur Amos Noyes Laboratory of Chemical Physics and the §Carl and Winfred Braun Laboratories of Chemistry and Molecular Biology, California Institute of Technology, Pasadena, California 91125; the ¶Department of Microbiology, Lund University, S-233 62 Lund, Sweden; and the ‖Molecular Biological Division, Veterans Administration Medical Center, University of California at San Francisco, San Francisco, California 94121

Electron paramagnetic resonance (EPR) studies of succinate:ubiquinone oxidoreductase (SQR) from *Paracoccus denitrificans* have been undertaken in the purified and membrane-bound states. Spectroscopic "signatures" accounting for the three iron-sulfur clusters (2Fe-2S, 3Fe-4S, and 4Fe-4S), cytochrome *b*, flavin, and protein-bound ubisemiquinone radicals have been obtained in air-oxidized, succinate-reduced, and dithionite-reduced preparations at 4–10 K. Spectra obtained at 170 K in the presence of excess succinate showed a signal typical of that of a flavin radical, but superimposed with another signal. The superimposed signal originated from two bound ubisemiquinones, as shown by spectral simulations. Power saturation measurements performed on the air-oxidized enzyme provided evidence for a weak magnetic dipolar interaction operating between the oxidized 3Fe-4S cluster and the oxidized cytochrome *b*. Power saturation experiments performed on the succinate- and dithionite-reduced forms of the enzyme demonstrated that the 4Fe-4S cluster is coupled weakly to both the 2Fe-2S and the 3Fe-4S clusters. Quantitative interpretation of these power saturation experiments has been achieved through redox calculations. They revealed that a spin-spin interaction between the reduced 3Fe-4S cluster and the cytochrome *b* (oxidized) may also exist. These findings form the first direct EPR evidence for a close proximity (2 nm) of the high potential 3Fe-4S cluster, situated in the succinate dehydrogenase part of the enzyme, and the low potential, low spin *b*-heme in the membrane anchor of the enzyme.

Succinate:ubiquinone oxidoreductase, SQR,[1] is the only membrane-bound enzyme in the tricarboxylic acid cycle. As "complex II," it performs the two-electron oxidation of succinate to produce fumarate, while transferring the electrons to quinone (Q) to yield quinol (QH_2). The reverse process is mediated by quinol:fumarate oxidoreductases (QFR), which occur in anaerobic and some facultative organisms. The two enzymes are related and are capable of catalyzing their respective reverse reactions under suitable conditions (1, 2).

SQR contains three or four polypeptides depending on the organism. The largest subunit, a flavoprotein, contains the dicarboxylate binding site and one flavin moiety (FAD); the latter is covalently bound in most cases. The iron-sulfur protein is intermediate in size and contains three iron-sulfur clusters of type 2Fe-2S, 4Fe-4S, and 3Fe-4S, often referred to as S-1, S-2, and S-3, respectively, in the case of SQR. These two hydrophilic subunits protrude into the cytosol (prokaryotic enzyme) or the mitochondrial matrix (eukaryotic enzyme), and together catalyze the succinate dehydrogenase activity of the enzyme. They are anchored to the membrane by one or two hydrophobic quinone polypeptides (QP), which may contain zero, one, or two *b*-heme(s). These anchoring subunits confer reactivity with the bound Qs; for SQR from bovine heart (3, 4) and a variety of higher plants (5), the existence of two Q sites has been established. SQR from *Paracoccus denitrificans* contains covalently bound FAD; the membrane anchor consists of two polypeptides with a mono-heme cytochrome *b* (6). Despite extensive efforts (for reviews see Refs. 1, 2, and 7), the electron-transfer pathway(s) and the mechanism of Q reduction in SQR remain controversial (1, 8, 9).

We chose to study the enzyme from *P. denitrificans* for the following reasons. The membrane-bound form of the *P. denitrificans* enzyme in whole cells is characterized by electron paramagnetic resonance (EPR) signals like those observed in mammalian mitochondria (10). *P. denitrificans* appears to be the closest bacterial homologue to this organelle (11, 12), and its SQR is amenable to molecular genetic techniques. The purification and basic biochemical properties of SQR from this bacterium have also been reported (6).

The air-oxidized, ferricyanide-oxidized, succinate- and dithionite-reduced forms of the enzyme have been investigated by EPR spectroscopy. Spectroscopic "signatures" accounting for each of the redox centers have been obtained at these different levels of reduction of the protein. EPR spectral simulations of the radical signals are consistent with two Q binding sites. An EPR signal characteristic of a *reduced* 3Fe-4S cluster, has been observed for the first time for SQR or QFR. In addition, we have

* This work was funded in part by National Institutes of Health Grants GM 22432 (to S. I. C.) and HL-16251 (to B. A. C. A.) and a grant from the Swedish Natural Science Research Council (to L. H.). The costs of publication of this article were defrayed in part by the payment of page charges. This article must therefore be hereby marked "*advertisement*" in accordance with 18 U.S.C. Section 1734 solely to indicate this fact.

** To whom correspondence should be addressed: Arthur Amos Noyes Laboratory of Chemical Physics 127–72, California Institute of Technology, Pasadena, CA 91125. Tel.: 626-395-6508; Fax: 626-578-0472; E-mail: ChanS@cco.caltech.edu.

[1] The abbreviations used are: SQR, succinate:ubiquinone oxidoreductase; E_m, redox midpoint potential; FAD, flavin adenine dinucleotide; $P_{1/2}$, half-saturation parameter; $Q_{2(6)(10)}$, ubiquinone-2(6)(10); S-1, 2Fe-2S cluster; S-2, 4Fe-4S cluster; S-3, 3Fe-4S cluster; Thesit, polyoxethylene (9) lauryl ether; Q, (ubi)quinone; $Q^{\cdot}$, (ubi)semiquinone; QFR; quinol fumarate oxidoreductase; QH_2, (ubi)quinol; QP, quinone polypeptides; MOPS, 4-morpholinepropanesulfonic acid.

analyzed quantitatively the power saturation and redox behavior of the S-3 center in the air-oxidized enzyme, and the S-3 and S-1 centers in the succinate-reduced enzyme. Taken together, we conclude that S-3 center and the *b*-heme are coupled magnetically in their oxidized states, and presumably in their respective reduced and oxidized states, as well.

EXPERIMENTAL PROCEDURES

Materials—Centricon ultrafiltration tubes were from Amicon Inc., Beverly, MA; dodecyl-β-D-maltoside was from Anatrace, Maumee, OH; 4-amino-2,2,6,6-tetramethyl-1-piperidinyloxyl, and Sephadex G-50 were purchased from Sigma Chemical Co.; polyethylene glycol *tert*-octylphenyl ether; Tris, Triton X-100, and polyoxethylene (9) lauryl ether (Tesit) were purchased from Boehringer Mannheim (Indianapolis, IN, or Mannheim, Germany); Amberlite XAD-2 adsorbent was from Serva, Heidelberg, Germany. All other reagents were of analytical reagent grade.

Cell Growth Conditions and Membrane Isolation—Growth of *P. denitrificans* (ATCC no. 13543) used for isolation of SQR was performed as described previously (13). Cells were harvested with a continuous flow centrifuge and frozen in liquid nitrogen as 200-g flat packs. Growth conditions for the PD1222/pPSD100 strain containing overproduced (~2-fold) SQR, its construction, and isolation of membranes from it, will be described elsewhere.[2]

Enzyme Purification—SQR was purified by thawing the stored cell packs using 150–200 g of material each time. The purification procedure was as described previously (6), with modifications similar to those described previously (14, 15). The enzyme was concentrated, and the salt and Triton X-100 concentrations of the final samples were reduced, the latter to ~0.05% (w/v), by repeated exchange in Centricon 100-kDa cutoff concentrators against 100 mM Hepes, pH 7.4. The final yield was 1–2 ml of 50–100 μM SQR. SQR from the PD1222/pPSD100 strain was purified in an identical fashion to that from the ATCC no. 13543 strain. The enzyme was considered sufficiently pure (>90%) for use in our experiments by criteria of optical spectra (negligible absorption due to hemes other than b_{557}) and SDS-polyacrylamide gel electrophoresis (6).

Analytical Procedures—Enzyme concentrations were determined by measuring the acid-nonextractable FAD content of the samples (16). Cytochrome *b* concentrations were determined from dithionite reduced-minus-oxidized difference spectra in a pyridine hemochrome assay mixture, using $\Delta\epsilon_{557-540}$ = 24.0 mM^{-1} cm^{-1} (17). The SQR activity was measured with a large excess of ubiquinone-2 (Q_2; 20 μM) and dichlorophenol-indophenol as the primary and terminal electron acceptors, respectively (6, 18); activation of the enzyme was achieved by incubating the enzyme (in Triton X-100) for 20 min at 298 K in 50 mM Tris buffer, 50 mM sodium succinate, 0.2 mM dodecyl-β-D-maltoside, pH 7.5. Typical turnover numbers (moles of succinate/mol of SQR) of the purified enzyme at 310 K were 300–350 s^{-1} based on the FAD concentrations of the samples (see also Ref. 6). Extraction of the protein-bound ubiquinone-10 (Q_{10}) was performed according to the procedure of Redfearn (19). Its concentration was determined using ubiquinone-6 (Q_6) as an internal standard for analysis by high performance liquid chromatography (275 nm) employing a C_{18} reverse-phase column and eluting with a solvent gradient starting at 25:75% water:acetonitrile and finishing at 100% acetonitrile.

EPR Sample Preparation—Samples stored at 193 K were thawed on ice and equilibrated with argon prior to freezing the samples in liquid nitrogen to remove oxygen from the system. Samples reduced with excess sodium succinate (35–100 mM, pH 7.4) were incubated for 45 min at 297–300 K; (sodium) dithionite-reduced samples (10 mM, pH 7.4) were incubated for 5 min at the same temperature. The succinate concentrations were varied between 35 and 100 mM to yield [succinate]/[SQR] ≈ 1300 ($E \approx -71$ mV, where E denotes solution potential; see below), for samples with different SQR concentrations; dithionite-reduced samples may be approximated by $E \leq -400$ mV. Succinate- and dithionite-reduced PD1222/pPSD100 membranes in 20 mM MOPS, 65 mM Hepes, pH 7.4, were treated identically, except for the addition of 2 mM KCN (final concentration) to these samples. Ferricyanide-oxidized SQR was obtained by incubating the sample with excess ferricyanide, which was subsequently removed by Sephadex G-50 column filtration. Samples, to which a 3-fold excess of (exogenous) Q_2 were added, were incubated for 5 min at 295 K and subsequently reduced with excess succinate, as described above. The QP were isolated from detergent-depleted SQR using perchlorate, essentially as described for the mammalian enzyme (20). The nonionic detergent Thesit (1.5% w/v) was removed from the SQR-detergent micelle mixture by adsorption to Amberlite XAD-2 beads.

EPR Methods—EPR spectra were recorded on a Varian E-109 X-band spectrometer equipped with a E-231 TE-102 rectangular cavity, and interfaced with an IBM personal computer for accumulation and digitization of the spectra. Sample temperature was controlled by a variable temperature helium flow cryostat system (Oxford Instruments). Spectral manipulation was performed using the program Labcalc on an IBM personal computer. Quantitation of the reduced S-1 and S-3 signal intensities (see Fig. 5) was performed by measuring peak heights (21); double integration of the digitized first-derivative spectra was performed in the case of the oxidized S-3 center (see Fig. 4). Spectra obtained at liquid helium temperatures (4–20 K) were base-line-corrected by subtracting spectra derived from a buffer-filled EPR tube under identical conditions. EPR signal line widths are given as peak-to-trough line widths under nonsaturating conditions. The combined spin concentrations of the radical signals due to FAD· and Q·][3] of the purified preparations (*solid lines* in Fig. 3, *A*, *C*, and *E*) have been determined using a 4-amino-2,2,6,6-tetramethyl-1-piperidinyloxyl standard under nonsaturating conditions.[4] EPR acquisition parameters are given in the figure legends; the number of scans taken per spectrum is one, unless mentioned otherwise.

Computational Procedures—EPR simulations of the composite FAD·-Q·signal (see Fig. 3) have been carried out using the program EPR, a modeling approach (F. Neese, University of Konstanz, Konstanz, Germany) on an IBM-compatible 486:50 MHz computer. The computer program uses first-order perturbation theory to simulate the EPR transitions as a function of the magnetic field (or frequency). This treatment was deemed to be sufficient, as the condition $A_0 \ll g_e\beta_e B$ is fulfilled for radicals; *i.e.* their hyperfine interactions are much smaller than their Zeeman interactions. Initial estimates of the anisotropy (axiality) in the g and hyperfine (A) matrices corresponding to the strongly coupled nitrogens of the FAD·, as well as the line widths (x, y, and z) of the FAD·, were obtained from those reported previously for flavoproteins. Proton hyperfine interactions and "g strain" were neglected (22). Initial simulations were generated using the option "Spectra series," which allows the simulator to test the effect of a particular EPR parameter on the (simulated) spectrum. When a satisfactory likening between the simulated and experimental spectrum was obtained, the g values and spectral weights of the Q· were "fine-tuned" using the option "Fit" (Simplex algorithm; see "Results" and the legend of Fig. 3 for further details).

Redox calculations used to estimate the percentage reduction of the redox centers within SQR in the presence of excess succinate (E ≈ −71 mV) and dithionite (E < −400 mV) were programmed in Mathematica (version 2.2.2) (23); the program is available from Dr. Chan upon request. The values of the redox midpoint potentials (E_m values) used in the calculations were those measured for the bovine heart enzyme,[5] unless mentioned otherwise[6]: $E_m^{FAD/FAD\cdot} = E_m^{FAD\cdot/FADH_2} = -71$ mV[6];

[2] M. Matsson, L. Hederstedt, and B. A. C. Ackrell, manuscript in preparation.

[3] We shall not distinguish here between the protonated and anionic forms of the FAD and Q semiquinones. In the bovine heart enzyme FAD· and Q· are predominantly in the protonated (49) and anionic (45) forms at physiological pH, respectively.

[4] The FAD·saturates at $P \geq 30$ μW in the *P. denitrificans* (A. R. Waldeck, H. K. Lee, and S. I. Chan, unpublished results) and bovine heart enzymes (37).

[5] Preliminary redox titrations (S.-C. Hung, A. R. Waldeck, and S. I. Chan, unpublished results) have shown that $E_m \approx 60$ mV for the *P. denitrificans* S-3 center, as in the bovine heart enzyme (26). A spin concentration of 90% is predicted for the S-1 center using the bovine-heart E_m value (−14 mV) (24); this compares well with the 88% measured experimentally (see "Results"). The resonances due to the S-2 center are elicited by dithionite reduction, but not by succinate reduction, as in the bovine heart protein ($E_m = -260$ mV) (25).

[6] The spin concentration of the composite FAD·-2Q· signal (Fig. 3) in succinate-reduced samples (E ≈ −71 mV) has been measured (see "EPR Methods") to amount to ~44% of the FAD (protein) concentrations for enzyme isolated from both strains. Using this estimate and the spectral weight of (Q_A· + Q_B·) with respect to FAD· (see legend of Fig. 3) we estimate 33% FAD·:FAD and 11% Q·:FAD (16% Q·:Q), and 36% FAD·:FAD and 8% Q·:FAD (≥4% Q·:Q) for samples isolated from the ATCC no. 13543 and PD1222/pPSD100 strain supplemented with a 3-fold excess of Q_2, respectively (see also legend of Fig. 3). Note that in the latter preparation *maximally* 2Q may bind. These spin concentrations are reproduced in the redox calculations using: $E_m^{FAD/FAD\cdot} = E_m^{FAD\cdot/FADH_2} = -71$ mV; and $E_m^{Q/Q\cdot} = 30$ mV; $E_m^{Q\text{-}QH_2} = -20$ mV, $E_m^{Fe^{3+}/Fe^{2+}}$

$E_m^{S-1_{ox}/S\text{-}1_{red}} = -14$ mV[5] (24); $E_m^{S\text{-}2_{ox}/S\text{-}2_{red}} = -260$ mV[5] (25); $E_m^{S\text{-}3_{ox}/S\text{-}3_{red}} = 60$ mV[5](26); $E_m^{Fe^{3+}/Fe^{2+}} = -175$ mV [6]; $E_m^{Q/Q\cdot} = 30$ mV[6]; $E_m^{Q/QH_2} = -20$ mV.[6]

The half-saturation parameter, $P_{1/2}$, was obtained from the EPR power-saturation data in Fig. 4*A* using curves generated in Mathematica (27, 28). The power saturation data in Figs. 4 and 5 were (also) analyzed using nonlinear least-squares regression onto the data of a semiempirical equation[7] (see also Table II) (29, 30) using the program Kaleidograph.

RESULTS

SQR from various eukaryotes and prokaryotes has been characterized by EPR in the membrane-bound and purified states (1). The bovine heart protein has been under intense investigation for many years (1, 2, 7), and should serve as an excellent point of departure for the *P. denitrificans* enzyme, because of its close evolutionary linkage (11). Also, the amino acid sequence similarity of the flavoprotein and iron-sulfur protein subunits is highly conserved between species (1).

We have focused on three issues in the present study: 1) EPR "fingerprinting" of membrane-bound and purified SQR, 2) investigating the EPR power saturation behaviors of the EPR signals of the iron-sulfur clusters centers in an attempt to derive structural information from their spin-relaxation behavior, and 3) performing redox calculations allowing quantitative interpretation of the experimental results.

Fingerprinting Spectra—EPR spectra of "as isolated" (*i.e.* air-oxidized), succinate-, and dithionite-reduced membranes of the SQR overproducing PD1222/pPSD100 strain are shown in Fig. 1. The spin-states of the redox centers of the enzyme at the three levels of reduction are given in Table I. For air-oxidized SQR, the almost isotropic resonance centered at g = 2.006 with a line width of 2.5 mT (Fig. 1*A*) is characteristic of a signal arising from the oxidized S-3 center (see also Fig. 2*A*) (1, 31, 32). The very broad trough superimposed onto the S-3 signal (see *inset* for absorption signal) forms part of a $g_y \approx 2.1$ component of the *b*-heme of SQR. This g value falls within the range of g_y values reported for low spin ferric hemes (33–35), and is the same as that for the purified enzyme (see below).

The above assignment to the *b*-heme was confirmed by the persistence of the signal in the succinate-reduced spectrum (Fig. 1*B*), as the E_m of the cytochrome *b* of the *P. denitrificans* enzyme[5] is much lower than that of the fumarate:succinate couple at pH 7.4 (5 mV) (36). Therefore, it is not reduced appreciably (~8%; data not shown) by succinate (see also Fig. 2, *A* and *B*). The g_z component, $3 < g_z < 4$, was also detectable, though barely (spectral region not shown, but see Fig. 2, *A* and *B*, for evidence of this feature). In addition, reduction with succinate elicited an almost axial ferredoxin-like spectrum for the S-1 center with $g_z = 2.01$, $g_y = 1.92$, and $g_x = 1.91$ (Fig. 1*B*); the g = 1.99 signal is characteristic of the FAD· of SQR (10, 37–39).

Upon addition of dithionite to the sample, broad resonances at g = 2.07 (positive maximum), and 1.86 and 1.77 (negative minima) due to the S-2 center appeared, superimposed onto those of the S-1 center, but those due to the FAD· and the *b*-heme disappeared (Fig. 1*C*). Assignment of the former features to the S-2 center was based on the fact that they were not elicited in the succinate-reduced spectrum, the S-2 center being a low-potential center ($E_m = -260$ mV in the bovine-heart enzyme) (25). Also, these signals are of very low intensity in SQR and fumarate reductase; this low intensity is thought to be due to spin-spin interactions with the other iron-sulfur clusters (1, 40) (see Fig. 5 for the relevant power saturation experiments).

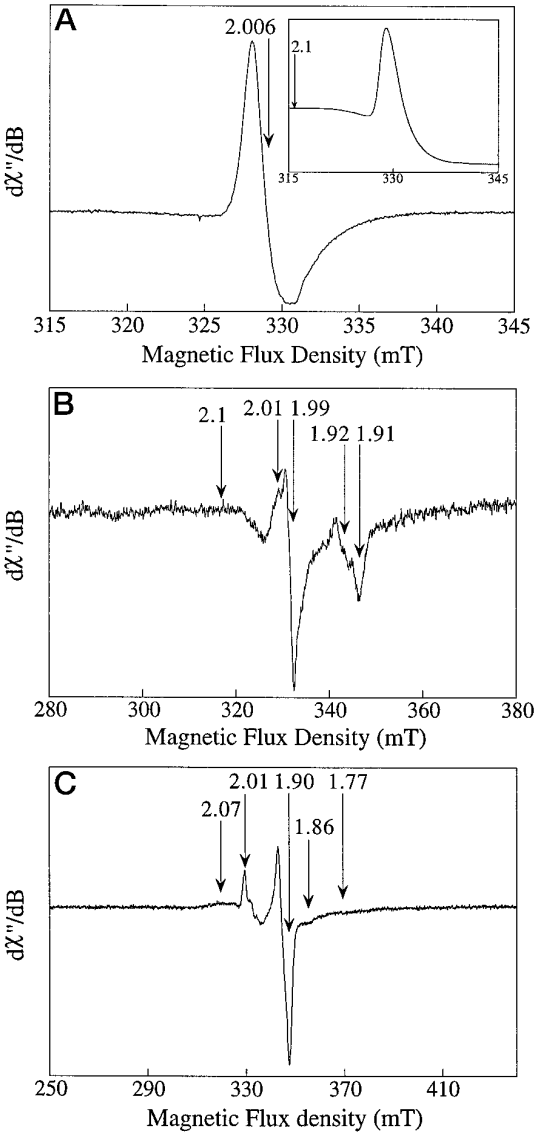

FIG. 1. **EPR spectra of membranes of the ~2-fold overproducing *P. denitrificans* strain, PD1222/pPSD100 [0.30 nmol of FAD/mg of protein (~2-fold overproduced); 3 mg of protein/ml].** *A*, no reductant added. EPR parameters: magnetic field, 330 mT; modulation amplitude, 0.5 mT; modulation frequency, 100 kHz; microwave power, 0.2 mW; microwave frequency, 9.236 GHz; field sweep rate, 0.17 mT s^{-1}; time constant, 0.064 s; temperature, 4 K. The *inset* shows the absorption (integrated) spectrum. *B*, succinate-reduced. EPR parameters were as in *A*, except for: modulation amplitude, 0.8 mT; field sweep rate, 0.21 mT s^{-1}; time constant, 0.25 s; number of scans, 2. *C*, dithionite-reduced. EPR parameters were as in *B*, except for: magnetic field, 350 mT; microwave power, 1 mW; temperature, 5 K. Relative gains of spectra *A*, *B*, and *C* were 1:7.5:2.3.

Fig. 2 depicts spectra recorded on purified SQR. Fig. 2*A* shows a nearly isotropic (g = 2.008) S-3 resonance (line width, 1.9 mT; see also Ref. 6) observed for the as isolated enzyme. The EPR signal intensities of the ferricyanide-oxidized and as isolated S-3 center were not significantly different; therefore, the 3Fe-4S cluster in as isolated samples of the enzyme was present in its oxidized state. The broad trough was (again) assigned to the g_y component of the *b*-heme (~2.1). The 0–300 mT region of the spectrum (*inset*) for the as isolated protein shows peaks at g = 5.9 and 4.2, and a very small one at g = 3.6; these features were assigned to high spin ferric hemes (presumably

= −175 mV, at pH 7.4 for the *P. denitrificans enzyme* (measured using redox mediators) (M. Matsson and L. Hederstedt, unpublished results).

[7] $I = K P^{1/2} [1 + (P/P_{1/2})]^{-b/2}$, where *I*, *K*, *P*, $P_{1/2}$, and *b* denote absorption integral or derivative intensity, proportionality constant, microwave power, half-saturation parameter, and inhomogeneity parameter, respectively (29, 30).

TABLE I

Spin states of the redox centers in SQR in the absence and presence of excess succinate and dithionite

The iron atoms in the iron-sulfur clusters are "high spin" ($S = 5/2$; see S-1); the heme-iron is "low spin" ($S = 1/2$). The total spin state (S_T) of the iron-sulfur clusters are calculated using antiferromagnetic interactions between the individual spins or "spin pairs" (subscripts 1, 2). The interactions between spin pairs are ferromagnetic; see *e.g.* S-2. Note that succinate is a mild reductant. Thus, addition of (excess) succinate to a sample of SQR elicits a "semireduced" (heterogeneous) state of the protein (see "Results").

Center	Air-oxidized	EPR	Succinate-reduced	EPR	Dithionite-reduced	EPR
FAD	S = 0	—	FAD·, $S = 1/2$	√	$FADH_2$, $S = 0$	—
S-1	Fe^{3+} (5/2)-Fe^{3+} (5/2) $S_T = 0$	—	Fe^{3+} (5/2)-Fe^{2+} (2) $S_T = 1/2$	√	Fe^{3+} (5/2)-Fe^{2+} (2) $S_T = 1/2$	√
S-2	Fe^{3+}-Fe^{2+}, $S_1 = 9/2$ Fe^{3+}-Fe^{2+}, $S_2 = 9/2$ $S_T = 0$	—	Fe^{3+}-Fe^{2+}, $S_1 = 9/2$ Fe^{3+}-Fe^{2+}, $S_2 = 9/2$ $S_T = 0$	—	Fe^{3+}-Fe^{2+}, $S_1 = 9/2$ Fe^{2+}-Fe^{2+}, $S_2 = 4$ $S_T = 1/2$	√
S-3	Fe^{3+}-Fe^{3+}, $S_1 = 0$ Fe^{3+}, $S_2 = 5/2$ $S_T = 5/2$[a]	√	Fe^{3+}-Fe^{2+}, $S_1 = 9/2$ Fe^{3+}, $S_2 = 5/2$ $S_T = 2$	√	Fe^{3+}-Fe^{2+}, $S_1 = 9/2$ Fe^{3+}, $S_2 = 5/2$ $S_T = 2$	√
b-heme	Fe^{3+} (1/2), $S = 1/2$	√	Fe^{3+} (1/2), $S = 1/2$	√	Fe^{2+}, $S = 0$	—
Q_A	$S = 0$	—	Q_A·, $S = 1/2$	√	Q_AH_2, $S = 0$	—
Q_B	$S = 0$	—	Q_B·, $S = 1/2$	√	Q_BH_2, $S = 0$	—

[a] Formally $S_T = 5/2$, but the Kramer's doublet ground state ($S_T = 1/2$) is the operative spin state at $T = 4$ K (Fig. 4*A*).

originating from slight contamination with terminal oxidases), adventitious iron, and a g_z component due to the *b*-heme, respectively.

The extent to which g anisotropy could be the cause of the low intensities of the *b*-heme g_z and g_y components (33, 34) was ascertained by comparing the intensities of the g_z components of low spin heme signals from different species. This effect was excluded because the g_z value of the *P. denitrificans b*-heme is comparable to that of the low potential *b*-heme of the bovine heart enzyme ($g_z = 3.46$; $E_m = -185$ mV) (41) and the high potential *b*-heme of the *Bacillus subtilis* succinate:menaquinone oxidoreductase ($g_z = 3.68$; $E_m = 65$ mV) (42). To determine whether the virtual EPR invisibility of the *b*-heme (g_z and g_y components) was due to relaxation-enhancement of this metal center by the S-3 center, or due to an extremely short *intrinsic* spin-lattice relaxation time, T_1, we prepared isolated QP. The EPR of the isolated QP (24 μM *b*-heme) showed a very small $g_z = 3.6$ signal (spectrum not shown), again in comparison with the g_z signals originating from the bovine heart enzyme and the *B. subtilis* succinate:menaquinone oxidoreductase, for comparable *b*-heme concentrations. Thus, it was concluded that the intrinsic T_1 of the cytochrome is very short.

Succinate-reduced purified SQR (Fig. 2*B*) gives rise to resonances at $g_z = 2.018$, $g_y = 1.920$, and $g_x = 1.910$ due to the reduced S-1 center. The $g_y \approx 2.1$ and $g_z \approx 3.6$ components due to the *b*-heme persist, as expected. A FAD· signal is observed at $g = 1.998$. The "shoulders" at $g = 1.990$ and 1.980 are attributed to Q· and scalar coupling of the FAD free radical electron to a strongly coupled nitrogen atom (22), respectively (see below; Fig. 3). The spectral feature due to the Q· in the membrane-bound enzyme was less readily detected due to the lower signal-to-noise ratio of that spectrum (see Fig. 1*B*). The *inset* in Fig. 2*B* shows a broad signal at $g = 12.6$ due to the reduced S-3 center. This spectral feature is consistent with a $\Delta M_S = 4$ transition within the $S_T = 2$ spin-manifold of the iron-sulfur cluster (43, 44) (see also "Discussion").

The dithionite-reduced enzyme (Fig. 2*C*) shows the spectral features expected from reduced centers S-1, at $g_z = 2.016$, $g_y = 1.922$, and $g_x = 1.910$, [see also (6)]; and S-2, at 2.27, 2.07, 2.05 (positive maxima), and 1.86 and 1.78 (negative minima). The g values of the S-1 center are virtually identical to those characterizing the iron-sulfur cluster in the succinate-reduced state of the enzyme (see above; Fig. 2*B*). This result suggests little or no reorganization of the ligands of the 2Fe-2S cluster upon reduction of the 4Fe-4S cluster. However, the succinate-reduced enzyme yielded ~0.88 spins/molecule compared with 1.00 for the dithionite-reduced sample, as measured from the intensities of the g_x-components of the 2Fe-2S cluster in the two samples. The integrated intensities of the resonances in the dithionite-reduced enzyme due to the S-1 and S-2 centers were approximately twice (2.15 ± 0.07; $n = 2$) that of the S-1 center alone. We take these findings as evidence for the fact that these centers are present in a 1: 1 molar ratio in the purified enzyme. The reduced S-3 center remained EPR-active ($g = 12.6$) as expected (see Table I) in the dithionite-reduced sample; the $g = 12.6$ signal has also been observed for the succinate- and dithionite-reduced membranes (spectra not shown).

EPR Spectral Simulations of the Radical Signals—SQR from bovine-heart (1, 3, 4, 45–47) and a variety of higher plants (5) binds tightly two Q's, of which the semi-quinone form is stabilized preferentially. In the bovine-heart enzyme a four-line spectrum is observed at $E \approx 100$ mV and T = 10–13 K (1, 46, 47), or during turnover (100 ms) (3). The spectral features appear to be best simulated by a dipolar-coupled Q·-Q·signal superimposed onto that of a non-interacting oxidized S-3 center (3, 45). However, evidence attesting to the possibility that the oxidized S-3 center ($M_S = \pm 1/2$; ground state Kramer's doublet; see Table I) interacts with the Q· has been provided by EPR simulation, and the fact that the spectroscopic features disappear concomitantly with reduction of the S-3 center (3). In our experiments we observed a signal reminiscent of Q· in the equilibrium succinate-reduced state of the *P. denitrificans* enzyme at 4 K (Fig. 2*B*); however, no observable splittings were present at this low temperature, as may be expected for the reduced state of the S-3 center ($S_T = 2$; see Table I). Therefore, we performed EPR spectral simulations of the $g = 2$ region of the succinate-reduced enzyme at 170 K (Fig. 3). At this temperature the resonances due to the S-1 center and the *b*-heme are conveniently broadened beyond detection.

We have simulated the experimental composite FAD·-Q·signal to establish whether the *P. denitrificans* enzyme binds one or two Q·. We have studied three different preparations from two strains. The first preparation (ATCC no. 13453 strain) contained 0.7 bound Q_{10}: FAD (see Fig. 3*A*); the second (PD1222/pPSD100 strain) contained 0.1 bound Q_{10}: FAD and was supplemented with a 3-fold stoichiometric excess (with respect to the FAD concentration) of exogenous Q_2 (see Fig. 3*C*); the control for this sample was a nonsupplemented sample containing 0.2 Q_{10}: FAD (see Fig. 3*E*). In the Q_2-supplemented preparation, we assume that the binding site(s) (is) are saturated with Q_2; in the former the Q_{10} is substoichiometric with respect to the enzyme, and distributes over the two Q sites (Q_A and Q_B; if present) according to their relative affinities ($1/K_d$ values), which are unknown at present.

To achieve our objective of assigning one or two Q sites to the *P. denitrificans* enzyme, without having an experimental spec-

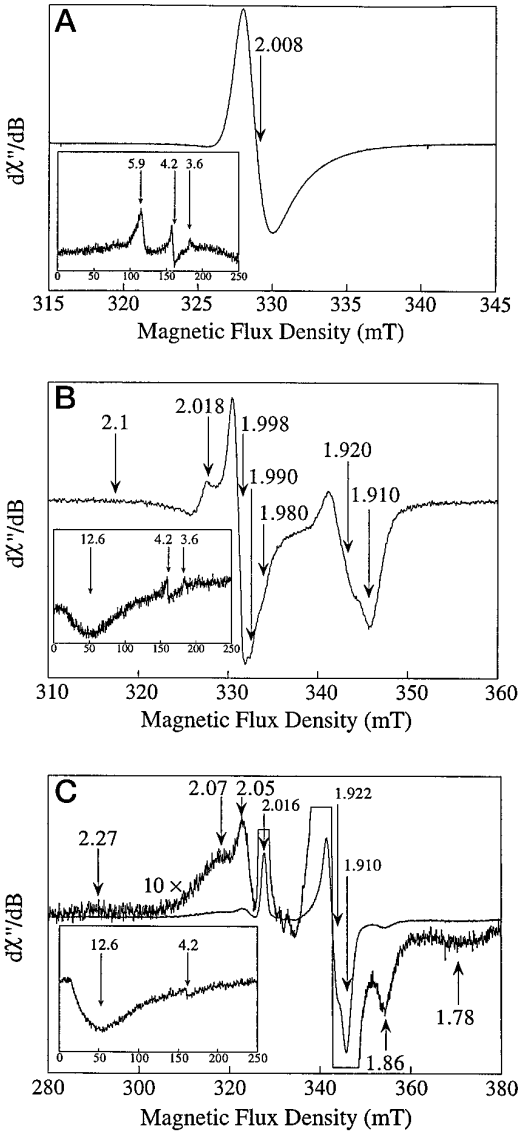

FIG. 2. **EPR spectra of purified *P. denitrificans* SQR (ATCC no. 13543 strain).** *A*, no reductant added (106 μM FAD; 79 μM *b*-heme). EPR parameters: magnetic field, 330 mT; modulation amplitude 0.5 mT; modulation frequency, 100 kHz; microwave power, 1.0 mW; microwave frequency, 9.234 GHz; field sweep rate, 0.08 mT s^{-1}; time constant, 0.064 s; temperature, 4 K. *B*, succinate-reduced SQR (77 μM FAD; 78 μM *b*-heme). EPR parameters were as in *A*, except for: field sweep rate, 0.21 mT s^{-1}; time constant, 0.13 s. *C*, dithionite-reduced; FAD and *b*-heme concentrations as in *B*. EPR parameters were as in *B*, except for: temperature, 10 K. Relative gains of spectra *A*, *B*, and *C* were 1:20:5. The *insets* show the entire 0–300-mT spectral regions. The relative gains of the insets to spectra *A*, *B*, and *C* were 15:1:1; the temperatures were 4, 8, and 4 K, respectively.

trum of the "pure" *P. denitrificans* FAD•signal (see below), we simulated the composite signal with a FAD• and either one or two superimposed Q•. Evidence for the g = 1.994 spectroscopic feature originating from Q• has come from comparison of the three samples with different Q contents. In accordance with the different Q content of these preparations, the g = 1.994 feature was altered (see legend to Fig. 3, *A*, *C*, and *E*).

We commenced by adjusting/fitting (see "Computational Procedures" for details) the EPR spectral parameters associated with the FAD• and one Q• (Fig. 3, *dashed-dotted line*) to the experimental FAD•-Q•spectrum (*solid line*) of the enzyme isolated from the ATCC no. 13543 strain; this simulation was then repeated with two Q• (Fig. 3*A*, *dotted line*). The hyperfine (*A*) constants, g values and line widths characterizing the EPR transitions of the FAD•, and the line widths of the Q•, for which a good fit to the experimental (FAD•-Q•) spectrum was obtained in both cases, were then kept constant (see Fig. 3 legend for their values). Thus, the EPR parameters that best characterized the *P. denitrificans* FAD• were decided upon and chosen to represent the pure FAD•signal (see *inset* of Fig. 3*A*; *top right-hand corner*). Further refinement (fitting; see "Computational Procedures") of the FAD•-1Q• and FAD•-2Q• simulations involved the g values and weights of the (two) Q•.

It is clear from Fig. 3*A* that the experimental spectrum of the ATCC no. 13543 strain is rather well simulated using either one or two superimposed Q•, although the FAD•-2Q• simulation appears superior (see *e.g.* the 329-mT region of the spectrum). However, to circumvent this problem, we subtracted the FAD• simulation from the experimental spectrum and from the FAD•-1Q• and FAD•-2Q• simulations. Thus, this procedure yields the features due to one Q• or two Q• only (see Fig. 3*B*), allowing us to discriminate more precisely between the FAD•-1Q• and FAD•-2Q• simulations. We conclude that the composite FAD•-Q•signal is best simulated using two Q•. The same procedure was then followed for the enzyme purified from the PD1222/pPSD100 strain in the presence of exogenous Q_2 (3-fold excess; Figs. 3*C*). Again, the simulated spectral features are better for the simulation with two Q• (*dotted lines* in Fig. 3, *C* and *D*). The experimental spectrum (*solid line*) and simulation (*dotted line*) for a similar preparation without added Q_2 is shown in Fig. 3*E*. The spectrum obtained on the membrane-bound enzyme (*solid line*) and its FAD•-2Q• simulation (*dotted line*) are shown in Fig. 3*F*.

The FAD• signals with their characteristic "wings," due to the strongly coupled N(5) and N(10) nitrogens (22, 48, 49) are observed in both the purified and membrane-bound preparations (*solid lines* in Fig. 3*A*, *C*, *E*, and *F*, respectively). The line width of the FAD• signal of the purified preparation is 1.15 mT. The "extreme shoulders" are separated by 5.4 mT and are due to the molecules with the magnetic field perpendicular to the plane of the FAD ring system. The values of the line width and the separation of the extreme shoulders are suggestive of the "red" (anionic) form of the radical (50). However, it is possible that the spectrum includes a contribution from proton hyperfine interactions (48). A mixed form at pH 7.4 would be consistent with a $pK_a = 8.0 \pm 0.2$ for the bovine heart enzyme (49).

Heme and Q Contents of the Purified Protein—The molar ratio of FAD to *b*-heme and Q_{10} in the enzyme purified from membranes of ATCC no. 13543 strain was $1:1.0 \pm 0.3:0.9 \pm 0.3$ (n = 11 and 5, respectively); thus, the preparations contained 0.9 ± 0.4 Q_{10} per *b*-heme. The number n represents measurements on different enzyme preparations. However, enzyme purified from membranes of PD1222/pPSD100 strain contained $1:1.3 \pm 0.4:0.1 \pm 0.1$ (n = 5) FAD: *b*-heme: Q_{10}; or 0.1 ± 0.1 Q_{10} per *b*-heme. The reason for the difference in the Q_{10} contents of SQR purified from the two strains is unknown at present.

EPR Power Saturation Behavior of the S-3 Center in the Air-oxidized Enzyme—The power saturation behavior of the (air) oxidized 3Fe-4S cluster has been measured in an attempt to deduce whether a dipolar interaction exists between this iron-sulfur cluster and the *b*-heme. Such magnetic coupling had been postulated (7), but EPR evidence for this interaction has been lacking.

Fig. 4*A* shows the EPR power saturation behavior of the S-3 signal in the air-oxidized enzyme. In this state of the enzyme, the cytochrome *b* is the only other center that is paramagnetic (see Table I). The $P_{1/2}$ values obtained from the computer-generated curves (see "Experimental Procedures") were 0.02, 32, and ~200 mW for the data recorded at 4, 10, and 20 K, respectively. The precision of the double-integrations could

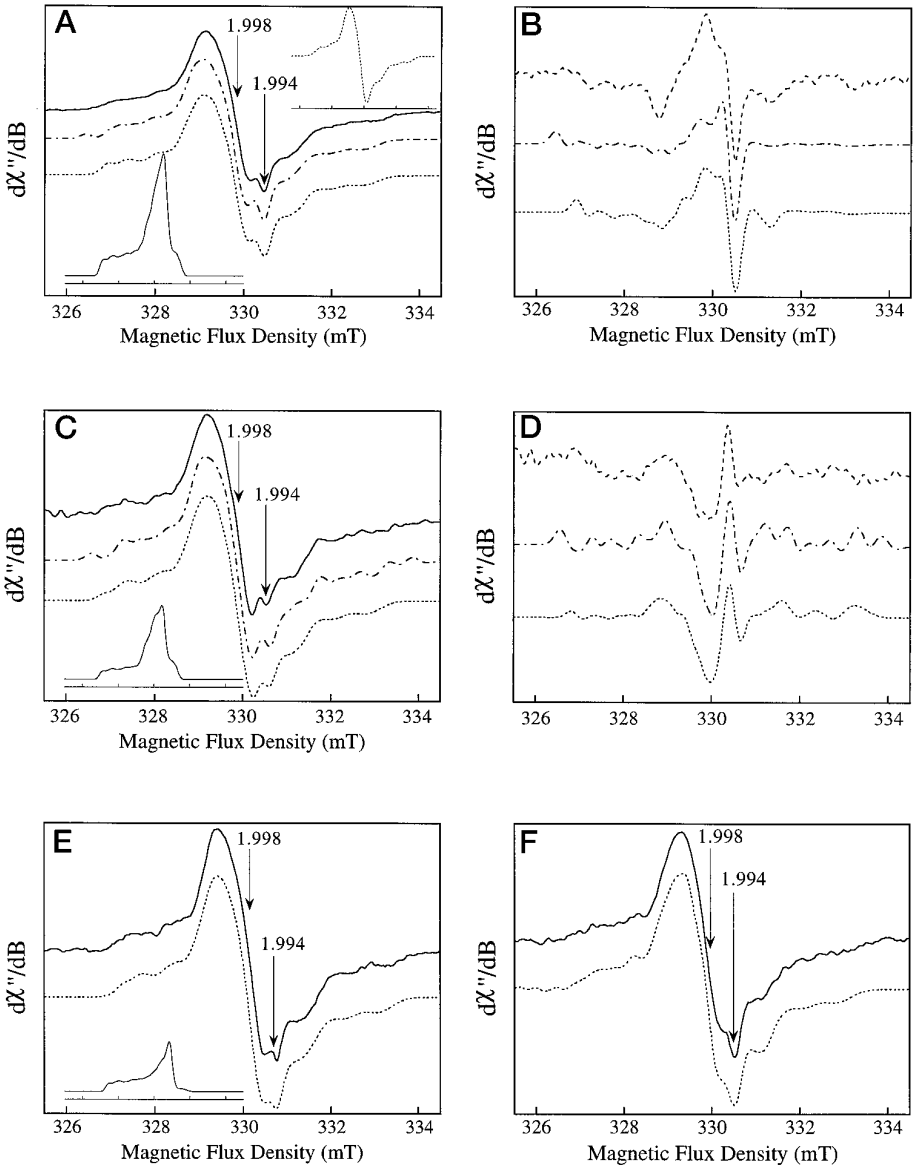

FIG. 3. **EPR spectra and spectral simulations of the g = 2 region of purified and membrane-bound succinate-reduced SQR at 170 K.** *A*, EPR spectrum (*solid line*) from purified SQR (average of two spectra; ATCC no. 13543 strain; 20 μM FAD; 22 μM *b*-heme; 13 μM Q_{10}) and simulations of a FAD$^{\bullet}$ with one (*dashed-dotted line*) or two superimposed Q$^{\bullet}$ (*dotted line*). The *inset* in the *top right-hand corner* depicts a simulation of the "pure" FAD$^{\bullet}$ (see "Results"). The *inset* in the *lower left-hand corner* shows the absorption signal of the two Q$^{\bullet}$ for the *dotted line*. The FAD$^{\bullet}$:FAD and Q$^{\bullet}$:Q molar ratios (see footnote 6) are 0.33 and 0.17, respectively. *B*, the effect of superposition of one and two Q$^{\bullet}$ signals onto that of the FAD$^{\bullet}$ for the spectra shown in *A*. *Dashed line*, experimental spectrum minus FAD$^{\bullet}$ simulation; *dashed-dotted line*, FAD$^{\bullet}$-1Q$^{\bullet}$ simulation minus FAD$^{\bullet}$ simulation; *dotted line*, FAD$^{\bullet}$-2Q$^{\bullet}$ simulation minus FAD$^{\bullet}$ simulation. *C*, EPR spectrum obtained on purified SQR samples from the PD1222/pPSD100 strain (39 μM FAD; 42 μM *b*-heme; 4 μM Q_{10}, supplemented with 117 μM Q_2; *solid line*) and spectral simulations of a FAD$^{\bullet}$ superimposed with one (*dashed-dotted line*) or two Q$^{\bullet}$ (*dotted line*). The *inset* in the *lower left-hand corner* shows the absorption signal of the two Q$^{\bullet}$ for the *dotted line*. The FAD$^{\bullet}$:FAD and Q$^{\bullet}$:Q molar ratios (see footnote 6) are 0.36 and $\geq$0.04, respectively. *D*, the effect of superposition of one and two Q$^{\bullet}$ signals onto that of the FAD$^{\bullet}$ (as in *B*) for the spectra shown in *C*. *E*, EPR spectrum obtained on SQR purified from the PD1222/pPSD100 strain (46 μM FAD; 58 μM *b*-heme; 11 μM Q_{10}; *solid line*) and spectral simulation of a FAD$^{\bullet}$ superimposed with two Q$^{\bullet}$ (*dotted line*). The *inset* in the *lower left-hand corner* shows the absorption signal of the two Q$^{\bullet}$ (*dotted line*). The FAD$^{\bullet}$:FAD and Q$^{\bullet}$:Q molar ratios (see footnote 6) are 0.38 and 0.25, respectively. The relative absorption integrals for the *insets* in *A*, *C*, and *E* are: 1.00, 0.60, and 0.43, respectively; they reflect the relative Q$^{\bullet}$($Q_A^{\bullet}$ + $Q_B^{\bullet}$) spin concentrations of the three preparations. *F*, EPR spectrum (*solid line*) and simulation (*dotted line*) of membrane-bound SQR (0.30 nmol of FAD/mg of protein; 3 mg of protein/ml). EPR parameters: magnetic field, 330 mT; modulation amplitude, 0.2 mT; modulation frequency, 100 kHz; microwave power, 0.5 mW (saturating conditions with respect to FAD$^{\bullet}$ (see footnote 4)); microwave frequency, 9.243 (*A*), 9.246 (*C* and *F*), 9.253 (*E*) GHz; field sweep rate, 0.167 mT s^{-1}; time constant, 0.250; number of scans, 100 (16 for *C* and *E*); temperature 170 K. Simulation parameters, FAD$^{\bullet}$ (*inset A*): $g_{x,y,z}$ = 2.0008, 2.0019, 2.0033; $A_{\parallel} - A_{\perp}$ = *21.8 MHz and 54.2 MHz for N(5) and N(10), respectively. Gaussian line width* (*x*, *y*, and *z*) = 0.454, 0.325, 0.366 mT; these parameters were kept constant. Q$^{\bullet}$: Gaussian line width (*x*, *y*, and *z*) = 0.155 mT (kept constant). Spectral weight of Q$^{\bullet}$ (with respect to FAD$^{\bullet}$) Q$^{\bullet}$ = 0.26, $g_{x,y,z}$ = 1.9982, 1.9986, 2.0229, for the *dashed-dotted line* in *A*. $Q_A^{\bullet}$ = 0.26, $g_{x,y,z}$ = 1.9978, 1.9988, 2.0199; $Q_B^{\bullet}$ = 0.09, $g_{x,y,z}$ = 1.9932, 2.0005, 2.0052, for the *dotted line* in *A*. Q$^{\bullet}$ = 0.16, $g_{x,y,z}$ = 1.9686, 1.9982, 2.0229, for the *dashed-dotted line* in *C*. $Q_A^{\bullet}$, weight = 0.14; $g_{x,y,z}$ = 1.9980, 1.9980, 2.0210; $Q_B^{\bullet}$, weight = 0.07; $g_{x,y,z}$ = 1.9932, 2.0005, 2.0052, for the *dotted line* in *C*. $Q_A^{\bullet}$, weight = 0.14; $g_{x,y,z}$ = 1.9984, 1.9988, 2.0200; $Q_B^{\bullet}$, weight = 0.01; $g_{x,y,z}$ = 1.9932, 2.0005, 2.0052, for the *dotted line* in *E*. $Q_A^{\bullet}$ = 0.24, $g_{x,y,z}$ = 1.9982, 1.9992, 2.0333; $Q_B^{\bullet}$ = 0.14, $g_{x,y,z}$ = 1.9943, 2.0016, 2.0051, for the *dotted line* in *F*.

have been compromised slightly by the superimposed g_y component from the *b*-heme for the 4 K data. The g_y and g_z components were broadened beyond detection for $T \geq 9$ K. Using the same analysis, the $P_{1/2}$ values of the S-3 center in the *B. subtilis* enzyme have been reported as 20 mW (5.5 K) and >300 mW (7 K), respectively (39, 51). Thus, interestingly, the spin

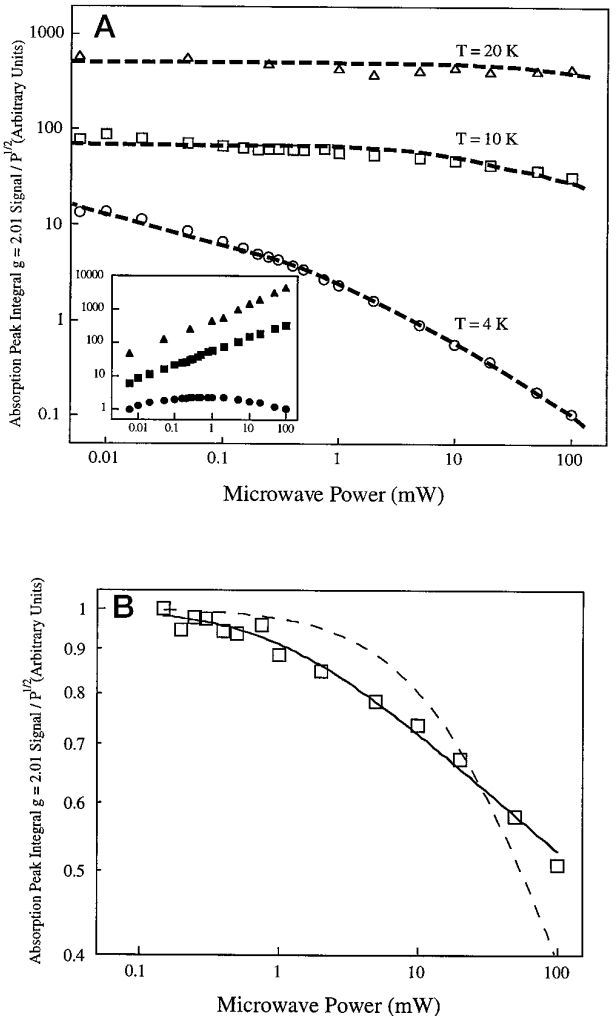

FIG. 4. *A*, EPR power saturation behavior of the oxidized S-3 center at 4, 10, and 20 K (ATCC no. 13543 strain). EPR parameters: magnetic field, 330 mT; modulation amplitude, 0.32 mT; modulation frequency, 100 kHz; microwave power, 0.2 mW; microwave frequency, 9.225 GHz; field sweep rate, 0.17 mT s^{-1}; time constant, 0.128 s. The "raw" data (absorption peak-integral *versus* microwave power) are shown in the *inset*. The $P_{1/2}$-values obtained from the simulated curves are given under "Results." *B*, best fits of an empirical equation describing the EPR power saturation (see footnote 7) to the 10 K data (*A*); see "Results" and Table II for parameter estimates.

relaxation of the 3Fe-4S cluster from the *P. denitrificans* enzyme is significantly slower than that of the *B. subtilis* enzyme, which contains *two* *b*-hemes (42).

Fig. 4*B* depicts the normalized 10 K power saturation data from Fig. 4*A* and "best fits" of a semiempirical equation describing the power saturation behavior.[7] The fits were obtained by "floating" the parameters $P_{1/2}$ and b (*solid curve*), or $P_{1/2}$ only ($b = 1.00$; *dashed curve*) in the regression analysis. The parameter estimates for the 10 K data were $P_{1/2} = 1.1 \pm 0.2$ mW and $b = 0.28 \pm 0.02$ for the *solid curve*, and $P_{1/2} = 18.1 \pm 3.4$ mW for the *dashed curve*; see Table II for estimates of the 4 K data.

The effect of the inhomogeneity parameter, b, is to flatten the curve in the region where part of the spins are being saturated; *i.e.* in the region where P is comparable to $P_{1/2}$. For a purely inhomogeneously broadened absorption signal (peak integral), $b = 1$; the purely homogeneously broadened case yields $b = 2$. The corresponding values for a derivative-type signal are $b = 1$ and $b = 3$, respectively (29). Thus, it is physically impossible for an isolated spin system to be characterized by $b < 1$, and such a scenario is therefore diagnostic of a dipolar interaction (30).

TABLE II

Parameter estimates obtained from best fits of the equation $I = K P^{1/2} [1 + (P/P_{1/2})]^{-b/2}$ *to the power saturation data* ($P > 0.1$ mW) *of the S-3 center in the air-oxidized enzyme, and the S-1 and S-3 centers in the succinate-(sred) and dithionite-reduced (dred) enzymes*

See footnote 7 for details.

Center	$P_{1/2}$ ± S.E.[a]	b ± S.E.	Absorption:derivative[b]	T (K)
	mW			
$S\text{-}3_{ox}$	0.21 ± 0.03	0.68 ± 0.01	Absorption	4
$S\text{-}3_{ox}$	1.1 ± 0.2	0.28 ± 0.02	Absorption	10
$S\text{-}3_{sred}$	6.0 ± 1.0	2.07 ± 0.13	Derivative	4
$S\text{-}3_{dred}$	8.2 ± 1.3	1.62 ± 0.08	Derivative	4
$S\text{-}1_{sred}$[c]	0.052 ± 0.018	1.13 ± 0.02	Derivative	4
$S\text{-}1_{dred}$[c]	0.58 ± 0.14	1.16 ± 0.04	Derivative	4
$S\text{-}1_{sred}$	3.9 ± 0.9	1.23 ± 0.07	Derivative	15
$S\text{-}1_{dred}$	25.1 ± 6.8	0.94 ± 0.10	Derivative	15

[a] S.E. denotes the standard error of the estimate.
[b] Absorption peak integral or derivative signal peak height (g_x component for the S-1 center).
[c] Fit to data for $P \geq 0.1$ mW.

As a result, the analysis provides evidence for enhancement of the spin relaxation of the S-3 center due to magnetic coupling with the *b*-heme.

Power Saturation Behavior of the S-3 and S-1 Centers in the Succinate- and Dithionite-reduced Enzymes—Two of the three Fe-S clusters are paramagnetic in both the succinate- and dithionite-reduced samples, namely S-1 ($S_T = 1/2$) and S-3 ($S_T = 2$). However, reduction of a sample of SQR with succinate or dithionite yields two distinct levels of reduction. As a result, the redox centers may be diamagnetic or paramagnetic in one or the other state of the enzyme depending on their E_m values (see Table I and "Computational Procedures," respectively). Thus, by measuring the power saturation behaviors of the S-1 and S-3 centers in succinate- and dithionite-reduced samples, we expect to observe relief of power saturation of these centers due to fast relaxing centers that are coupled to them.

Fig. 5 depicts the EPR power saturation behavior of the reduced S-3 ($g = 12.6$ (*A*) and S-1 ($g_x = 1.9$ (*B*), centers in the presence of excess succinate (■) and dithionite (and succinate) (□) at 4 K. The *inset* in *B* shows data obtained on the S-1 center at 15 K. The dithionite-reduced samples were noted to be less readily power-saturated than their succinate-reduced counterparts. Also, the extent of relief of power saturation is more pronounced for the S-1 center than for the S-3 center (see below). Since reduction of the S-2 center with dithionite causes it to be paramagnetic (see Fig. 2*C* and Table I), the data demonstrate magnetic couplings between the S-3 and S-2 centers (*A*), and S-1 and S-2 centers (*B*).

In the above we have assumed that the center under observation in the power saturation experiment is the only paramagnetic center in the succinate-reduced enzyme, and that the S-2 center and the center under observation are the only paramagnetic centers in the dithionite-reduced enzyme. However, this is not the case for SQR (see Table I). To ascertain the effects of other paramagnetic centers, we therefore calculated the fractions of protein molecules that contained the center under study, as well as each of the other paramagnetic centers, both for the succinate- and dithionite-reduced states of the enzyme (see below; "Computational Procedures"). Armed with these results, we reconsider our interpretation of the power saturation curves in Fig. 5, *A* and *B*.

When changing from the succinate-reduced state to the dithionite-reduced state of the enzyme, the S-3 center remains reduced, and the *b*-heme and the S-2 center become reduced (see Table I). The species consisting of $S\text{-}3_{red}$ and oxidized *b*-heme (Fe^{3+}), and $S\text{-}3_{red}$ and $S\text{-}2_{red}$, decrease and increase by 98 and 100%, respectively (subscript red denotes reduced); thus, $S\text{-}2_{red}$ "substitutes" for Fe^{3+} when changing E from −71

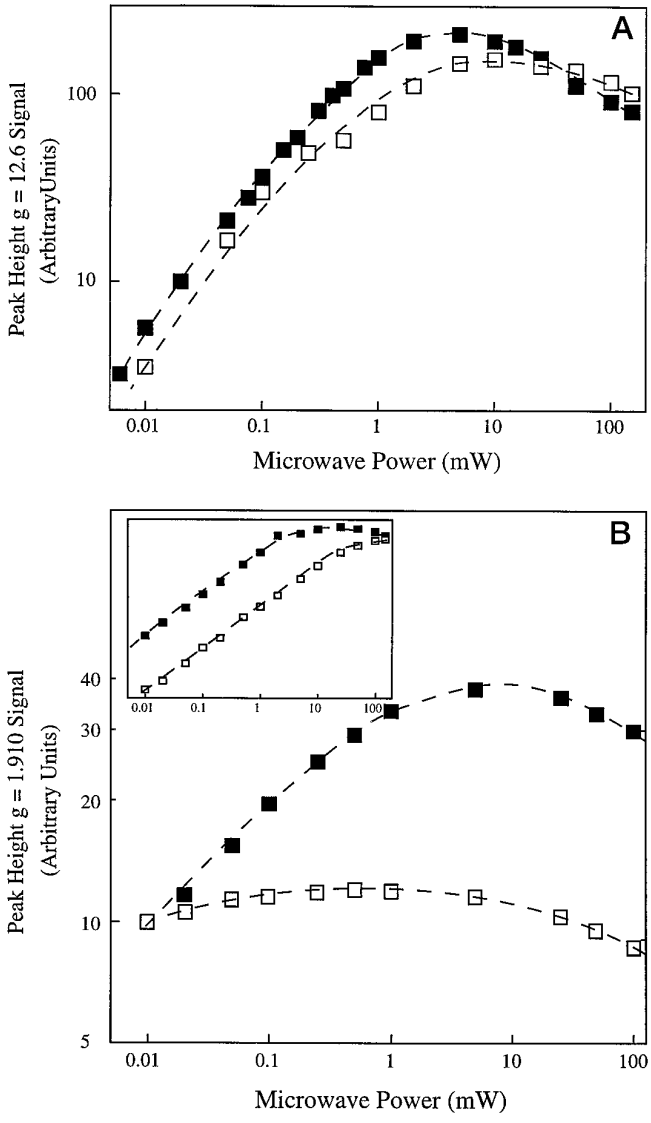

FIG. 5. **EPR power-saturation behavior of the reduced S-3 (*A*) and S-1 (*B*) centers (ATCC No. 13543 strain).** The symbols ■ and □ denote succinate- and dithionite-reduced enzyme, respectively. *A*, EPR parameters: magnetic field, 50 mT; modulation amplitude, 2.0 mT; modulation frequency, 100 kHz; microwave frequency, 9.229 GHz; field sweep rate, 0.83 mT s^{-1}; time constant, 0.25; temperature, 4 K. *B*, EPR parameters: magnetic field, 345 mT; modulation amplitude, 0.5 mT; modulation frequency, 100 kHz; microwave frequency, 9.229 GHz; field sweep rate, 0.33 mT s^{-1}; time constant, 0.128, temperature, 4 K. *Inset* (PD1222/pPSD100 strain), identical EPR parameters, except for temperature, 15 K. The *dashed lines* serve to guide the eye; see Table II for estimates of $P_{1/2}$ and *b*.

mV to < −400 mV in the experiment in Fig. 5*A*.

The percentages of enzyme molecules consisting of S-3_{red} and any of S-1_{red}, Q˙, or FAD˙ also change upon reduction of the succinate-reduced sample with dithionite (10, 11, and 33%, respectively). However, these changes are inconsequential to the analysis, as radicals are not capable of relaxing a metal center, and the S-1 center relaxes much slower than the S-3 center at 4 K (see Table II).

When changing from the succinate-reduced state to the dithionite-reduced state of the enzyme the protein species containing S-1_{red} and Fe^{3+}, and S-1_{red} and S-2_{red} decrease by 89% and increase by 100%, respectively. Thus, in the experiment in Fig. 5*B* these enzyme species are also affected most by reduction of the succinate-reduced sample with dithionite.

Enzyme molecules consisting of S-1_{red} and either FAD˙or Q˙ (30 and 10%, respectively), are (again) affected to a lesser extent, and (again) the radicals are not capable of relaxing the iron-sulfur clusters, the 2Fe-2S cluster in this case. The percentage concentration of the protein species containing S-1_{red} and S-3_{ox} remains essentially unchanged, and therefore, it could not have caused the relief of power saturation observed in the experiment, either at 4 or 15 K (*inset*). However, the species containing S-1_{red} (S_T = 1/2) and S-3_{red} (S_T = 2) increases by 10% upon dithionite reduction of the sample. Thus, there is a possibility that there is a minor contribution to the relief of power saturation from relaxation enhancement of S-1_{red} by S-3_{red} through a putative magnetic interaction (52, 53). There is precedent for an interaction between the oxidized S-3 center (S_T = 1/2) and the reduced S-1 center in *Micrococcus luteus* (54) and *B. subtilis* (55).

Taken together, the *minor* relief of power saturation of the succinate-reduced S-3 center upon reduction of the sample with dithionite (Fig. 5*A*) may be due to substituting the *b*-heme with the S-2 center as the interacting partner. However, it remains possible that the S-2 center is more efficient at relaxing the S-1 center than it is at relaxing the S-3 center. This scenario would also result in minor relief of power saturation.

In the case of the S-1 center (Fig. 5*B*), there is *substantial* relief of power saturation due to the S-2 center becoming paramagnetic in the dithionite-reduced state of the enzyme. This observation suggests that the 2Fe-2S cluster is not coupled to the *b*-heme. This finding is consistent with the topology of this iron-sulfur cluster within the iron-sulfur protein (see Fig. 10 in Ref. 7).

DISCUSSION

In the present work we have characterized the EPR signals observed in air- and ferricyanide-oxidized, and succinate- and dithionite-reduced SQR purified from *P. denitrificans*. We have focused in particular on elucidating the magnetic interactions operating between the metal centers and simulating the EPR signals from the radicals.

EPR Fingerprinting Studies—Bacterial respiratory chains are generally dominated by features originating from SQR (44, 56). As a general comparison, we obtained spectra of membranes from a *P. denitrificans* strain (PD1222/pPSD100) overproducing SQR (Figs. 1 and 3*F*). These spectra were highly similar to those of the purified enzyme (Figs. 2 and 3*A*; ATCC no. 13543 strain) at the three levels of reduction of the protein. Therefore, we conclude that the purified enzyme has been prepared in its native state.

EPR Spectral Simulations of the Radical Signals—The two Q˙ in the FAD˙-2Q˙ simulations were taken to be isolated spins; *i.e.* no dipolar interaction between them needs to be included. Since a dipolar-coupled signal is observed for the Q˙ pair in the bovine heart enzyme (3, 4, 45–47, 57) and that of a variety of higher plants (5), it may be expected that such an interaction would also operate in the *P. denitrificans* enzyme. However, we predict a maximal spin concentration of 55% Q˙: FAD at E = 5 mV (*i.e.* $(E_m^{Q/Q\cdot} - E_m^{Q\cdot/QH_2})/2$) instead of 11%[5] as determined from the spin-concentration and EPR simulations of the ATCC no. 13543 strain. Thus, (redox) poising the enzyme with a large excess of succinate ($E \approx -71$ mV) is most likely not optimal for eliciting substantial spin concentrations of Q˙. This may also be the main reason for the signal being well simulated by two *non*interacting Q. In addition, the sample with the full complement of Q (Q_2) has less Q˙:Q (see Fig. 3, *A* and *C*) than the sample with 0.7 Q (Q_{10}):FAD. This result suggests that the enzyme has greater affinity (lower K_d) for the native Q_{10}.

Power Saturation of the S-3 Center in the Air-oxidized Enzyme—The analysis used in Fig. 4*B* provides evidence for a magnetic interaction between the cytochrome *b* and the S-3

center in their respective oxidized states; see Results. In the following, we shall argue that Fig. 4*A* also presents evidence for the interaction.

The analysis used in Fig. 4*A* corrects for extended sample geometry, unlike the one used in Fig. 4*B*. That is, the magnetic component of the microwave magnetic field is not constant inside the EPR cavity, and this is corrected for by sampling (averaging) the field over the dimensions of the cavity. It is evident from Fig. 4*A* that inclusion of such a correction term in the (analytical) equation (27, 28) accommodates some of the "flattening" (inhomogeneity) effect for $P \approx P_{1/2}$ (see also "Results"). However, upon closer inspection of the 10 K data, it becomes clear that it does so less well than the empirical fit[6] with $b = 0.3$ (*solid line* in Fig. 4*B*). Notably, however, the curve to the 10 K data in Fig. 4*A* was simulated assuming a 100% gaussian distribution for the individual spin packet line shapes; *i.e.* 100% inhomogeneous broadening. Using <100% inhomogeneous broadening resulted in a worse fit. In this regard, it is worth considering that one phenomenon giving rise to inhomogeneous broadening, is a dipole-dipole interaction between nonidentical centers (27). Thus, taken together, both analyses provide evidence for the fact that the spin relaxation of the oxidized 3Fe-4S is enhanced by a (weak) dipolar interaction provided by the fast relaxing spin of the *b*-heme (oxidized).

Previous indirect evidence obtained on the bovine heart enzyme also points to the S-3 center being proximal to the *b*-heme. The sensitivity of the S-3 center in succinate dehydrogenase to molecular oxygen (58) is consistent with our evidence for a magnetic interaction between the *b*-heme and the 3Fe-4S cluster.

Estimation of the Intercenter Distance between the S-3 Center and the b-Heme in the Air-oxidized Enzyme—From the absence of observable (~0.5 mT) splittings in the g = 2.01 signal, a lower limit of ~1.8 nm between the 3Fe-4S cluster and the *b*-heme may be estimated assuming dipolar coupling[8] (7, 52). However, these splittings may be obscured due to the large anisotropy of the *b*-heme signal and the relative orientations of the principal axes of the two centers with respect to each other and the magnetic field. A significant exchange-interaction (J) may be excluded, as it could not have resulted in a "signature" signal for an oxidized 3Fe-4S cluster, namely g_{av}-value = 2.01 (where $g_{av} = (g_x + g_y + g_z)/3$) (59). Therefore, we estimate a distance (r) of $0.5 < r \leq 2$ nm.

The Magnitude of the Zero Field Splitting Parameters of the S-3 Center in the Reduced Enzyme—In samples reduced with excess succinate and dithionite, we observed for the first time for SQR or QFR a spectral feature originating from a reduced 3Fe-4S cluster ($S_T = 2$; see Table I). The resonance is observed at low-field ($g \approx 13$), and is consistent with a $\Delta M_S = 4$ transition within the reduced cluster (43). Observation of (part of) such a "quarter-field" resonance at X band implies that $\Delta \approx 0.3$ cm^{-1}, where Δ is the energy splitting between the $M_S = \pm 2$ ground state levels (60, 61). From similar observations on natural and synthetic cuboidal 3Fe-4S clusters (see Table VI in Ref. 62) and a suitable spin hamiltonian,[9] we may estimate $D \approx -2.5$ cm^{-1} and $E/D = 0.20-0.25$, respectively, where D and E denote the axial and rhombic zero field splitting parameters, respectively.

Power Saturation Behavior of the S-3 and S-1 Centers in the Succinate- and Dithionite-reduced Enzymes—The relief of power saturation of the S-3 and S-1 centers upon reduction of the succinate-reduced samples with dithionite (Fig. 5) has been taken as evidence for weak dipolar interactions between the centers in question and the S-2 center. Similar decreases in the T_1 values of succinate-reduced S-1 centers upon reduction with dithionite have been observed in bovine heart SQR (38), *B. subtilis* succinate:menaquinone reductase (39), and *Escherichia coli* fumarate reductase (40). A magnetic interaction between the reduced S-2 and S-3 centers has also been inferred from soluble (succinate dehydrogenase) preparations partially or almost completely devoid of 3Fe-4S cluster (1).

Conclusions—In this work we have shown that the fingerprinting spectra obtained on the *P. denitrificans* enzyme are largely similar to those of the bovine heart enzyme, with the exception of the $Q^{\cdot}$ signals. It has been demonstrated by EPR simulation that *P. denitrificans* SQR binds two $Q^{\cdot}$; however, their E_m values are ~100 mV lower than in the bovine heart enzyme. A weak dipolar interaction between the S-3 center and the *b*-heme in the oxidized enzyme has been revealed by power saturation experiments. A similar magnetic interaction may exist in the reduced enzyme, as revealed by power-saturation data obtained on the succinate- and dithionite-reduced samples and redox calculations. This is the first evidence obtained on the intact complex for a close proximity of these two centers. Taken together, these EPR data are entirely consistent with the topological picture postulated by Ohnishi (see Fig. 10 in Ref. 7). That is, the three iron-sulfur clusters are located in the iron-sulfur protein within 2 nm of each other, and the S-3 center is the iron-sulfur cluster in closest proximity (≤2 nm) to the *b*-heme in the QP.

Acknowledgment—We thank the late Dr. Vladimir Sled for valuable correspondence. Drs. Siegfried Musser and Brian Schultz are thanked for stimulating discussions and advice with EPR simulations, respectively.

REFERENCES

1. Ackrell, B. A. C., Johnson, M. K., Gunsalus, R. P., and Cecchini, G. (1992) in *Chemistry and Biochemistry of Flavoenzymes* (Müller, F., eds) pp. 229–297, CRC Press, Boca Raton, FL
2. Hederstedt, L., and Ohnishi, T. (1992) in *Molecular Mechanisms in Bioenergetics* (Ernster, L., eds) pp. 163–198, Elsevier Science Publishers, Amsterdam
3. Ruzicka, F. J., Beinert, H., Schepler, K. L., Dunham, W. R., and Sands, R. (1975) *Proc. Natl Acad. Sci. U.S.A.* **72,** 2886–2890
4. Ingledew, W. J., Salerno, J. C., and Ohnishi, T. (1976) *Arch. Biochem. Biophys.* **177,** 176–184
5. Rich, P. R., Moore, A. L., Ingledew, W. J., and Bonner, W. D. (1977) *Biochim. Biophys. Acta* **462,** 501–514
6. Pennoyer, J. D., Ohnishi, T., and Trumpower, B. L. (1988) *Biochim. Biophys. Acta* **935,** 195–207
7. Ohnishi, T. (1987) *Curr. Top. Bioenerg.* **15,** 37–65
8. Cammack, R., Maguire, J. J., and Ackrell, B. A. C. (1987) in *Cytochrome Systems. Molecular Biology and Bioenergetics* (Papa, S., Chance, B., and Ernster, L., eds) pp. 485–491, Plenum Press, New York
9. Salerno, J. C. (1991) *Biochem. Soc. Trans.* **19,** 599–605
10. Albracht, S. P., Van Verseveld, H. W., Hagen, W. R., and Kalkman, M. L. (1980) *Biochim. Biophys. Acta* **593,** 173–186
11. Yang, D., Oyaizu, Y., Oyaizu, H., Olsen, G. J., and Woese, C. R. (1985) *Proc. Natl Acad. Sci. U.S.A.* **82,** 4443–4447
12. John, P., and Whatley, F. R. (1975) *Nature* **254,** 495–498
13. Stowell, M. H. B., Larsen, R. W., Winkler, J. R., Rees, D. C., and Chan, S. I. (1993) *J. Phys. Chem.* **97,** 3054–3057
14. Berry, E. A., and Trumpower, B. L. (1985) *J. Biol. Chem.* **260,** 2458–2467
15. Steffens, G. C. M., Pascual, E., and Buse, G. (1990) *J. Chromatogr.* **521,** 291–299
16. Wilson, D. F., and King, T. E. (1964) *J. Biol. Chem.* **239,** 2683–2690
17. Berry, E. A., and Trumpower, B. L. (1987) *Anal. Biochem.* **161,** 1–15
18. Trumpower, B. L., and Simmons, Z. (1979) *J. Biol. Chem.* **254,** 4608–4616
19. Redfearn, E. R. (1967) *Methods Enzymol.* **10,** 381–384
20. Hatefi, Y., and Galante, Y. M. (1980) *J. Biol. Chem.* **255,** 5530–5537
21. Orme-Johnson, N. R., and Orme-Johnson, W. H. (1978) *Methods Enzymol.* 252–257

[8] $H_{eff} = \pm 3/2\ \mu_0/r^3\ (1 - 3\cos^2\theta)$, where H_{eff} is the (classical) effective magnetic field splitting by two interacting equivalent electron dipole moments, and μ_0 denotes the permeability of vacuum (52). Thus, we have $H_{eff} \propto 3/2\ \mu_0/r^3$ from which an intercenter distance of ~1.8 nm is estimated for splittings of 0.5 mT.

[9] $\hat{H}_e = D[\hat{S}_Z^2 - 1/3\ S(S+1) + E/D(\hat{S}_x^2 + \hat{S}_y^2)] + \beta_e B \cdot g_e \cdot \hat{S}$. Assuming the Zeeman interaction is isotropic ($g_e \approx 2$), and $|D| \gg g_e\ \beta_e\ B$, each Kramers' doublet may be treated separately, assuming a "fictitious" spin $\hat{S}' = 1/2$. The splitting Δ of the levels lowest in energy ($M_s = \pm 2$) puts a constraint on the axial (D) and rhombic (E) zero field splitting parameters, namely $\Delta = 2D\ (x^{1/2} - 1)$, where $x = 1 + 3\ (E/D)^2$ (60–62).

22. Eriksson, L. E. G., and Ehrenberg, A. (1973) *Biochim. Biophys. Acta* **293,** 57–66
23. Wolfram, S. (1994) *Mathematica*, Addison-Wesley, Redwood City, CA
24. Bonomi, F., Pagani, S., Cerleti, P., and Giori, C. (1983) *Eur. J. Biochem.* **134,** 439–445
25. Maguire, J. J., Johnson, M. K., Morningstar, J. E., Ackrell, B. A. C., and Kearney, E. B. (1985) *J. Biol. Chem.* **260,** 10909–10912
26. Ohnishi, T., Lim, J., Winter, D. B., and King, T. E. (1976) *J. Biol. Chem.* **251,** 2105–2109
27. Blum, H., and Ohnishi, T. (1980) *Biochim. Biophys. Acta* **621,** 9–18
28. Castner, T. G. (1959) *Physiol. Rev.* **115,** 1506–1515
29. Sahlin, M., Gräslund, A., and Ehrenberg, A. (1986) *J. Magn. Reson.* **67,** 135–137
30. Galli, C., Innes, J. B., Hirsh, D. J., and Brudvig, G. W. (1996) *J. Magn. Reson.* **B 110,** 284–287
31. Ackrell, B. A. C., Kearney, E. B., Mims, W. B., Peisach, J., and Beinert, H. (1984) *J. Biol. Chem.* **259,** 4015–4018
32. Morningstar, J. E., Johnson, M. K., Cecchini, G., Ackrell, B. A. C., and Kearney, E. B. (1985) *J. Biol. Chem* **260,** 13631–13638
33. De Vries, S., and Albracht, S. P. J. (1979) *Biochim. Biophys. Acta* **546,** 334–340
34. Salerno, J. C. (1984) *J. Biol. Chem.* **259,** 2331–2336
35. Moore, G. R., Williams, R. J. P., Peterson, J., Thomson, A. J., and Mathews, F. S. (1985) *Biochim. Biophys. Acta* **829,** 83–96
36. Sucheta, A., Ackrell, B. A. C., Cochran, B., and Armstrong, F. A. (1992) *Nature* **356,** 361–362
37. Beinert, H., Ackrell, B. A. C., Kearney, E. B., and Singer, T. P. (1975) *Eur. J. Biochem.* **54,** 185–194
38. Ohnishi, T., Salerno, J. C., Winter, D. B., Lim, J., Yu, C. A., Yu, L., and King, T. E. (1976) *J. Biol. Chem.* **251,** 2094–2104
39. Hederstedt, L., Maguire, J. J., Waring, A. J., and Ohnishi, T. (1985) *J. Biol. Chem.* **260,** 5554–5562
40. Johnson, M. K., Morningstar, J. E., Cecchini, G., and Ackrell, B. A. C. (1985) *Biochem. Biophys. Res. Commun.* **131,** 756–762
41. Yu, L., Xu, J.-X., Haley, P. E., and Yu, C.-A. (1987) *J. Biol. Chem.* **262,** 1137–1143
42. Hägerhäll, C., Aasa, R., von Wachtenfeldt, C., and Hederstedt, L. (1992) *Biochemistry* **31,** 7411–7421
43. Hagen, W. R., Dunham, W. R., Johnson, M. K., and Fee, J. A. (1985) *Biochim. Biophys. Acta* **828,** 369–374
44. Anemüller, S., Hettmann, T., Moll, R., Teixeira, M., and Schäfer, G. (1995) *Eur. J. Biochem.* **232,** 563–568
45. Salerno, J. C., and Ohnishi, T. (1980) *Biochem. J.* **192,** 769–781
46. Ohnishi, T., and Trumpower, B. L. (1980) *J. Biol. Chem.* **255,** 3278–3284
47. Miki, T., Yu, L., and Yu, C. (1992) *Arch. Biochem. Biophys.* **293,** 61–66
48. Hyde, J. S., Eriksson, L. E. G., and Ehrenberg, A. (1970) *Biochim. Biophys. Acta* **222,** 688–692
49. Ohnishi, T., King, T. E., Salerno, J. C., Blum, H., Bowyer, J. R., and Maida, T. (1981) *J. Biol. Chem.* **256,** 5577–5582
50. Edmondson, D. E., Ackrell, B. A. C., and Kearney, E. B. (1981) *Arch. Biochem. Biophys.* **208,** 69–74
51. Hägerhäll, C., Sled, V., Hederstedt, L., and Ohnishi, T. (1995) *Biochim. Biophys. Acta* **1229,** 356–362
52. Abragam, A., and Bleaney, B. (1986) *Electron Paramagnetic Resonance of Transition Ions*, Dover Publications, Inc., New York
53. Cammack, R., Williams, R., Guigliarelli, B., More, C., and Bertrand, B. (1994) *Biochem. Soc. Trans.* **22,** 721–725
54. Crowe, B. A., Owen, P., Patil, D. S., and Cammack, R. (1983) *Eur. J. Biochem.* **137,** 191–196
55. Maguire, J. J., Magnusson, K., and Hederstedt, L. (1986) *Biochemistry* **25,** 5202–5208
56. Hurst, J. K., Barrette, W. C., Michel, B. R., and Rosen, H. (1991) *Eur. J. Biochem.* **202,** 1275–1282
57. Salerno, J. C., Harmon, H. J., Blum, H., Leigh, J. S., and Ohnishi, T. (1977) *FEBS Lett.* **82,** 179–182
58. Ohnishi, T., Winter, D. B., Lim, J., and King, T. E. (1974) *Biochem. Biophys. Res. Commun.* **61,** 1017–1025
59. Beinert, H., and Thomson, A. J. (1983) *Arch. Biochem. Biohys.* **222,** 333–361
60. Moura, I., Macedo, A., and Moura, J. J. G. (1989) in *Advanced EPR. Applications in biology and biochemistry* (Hoff, A. J., eds) pp. 813–834, Elsevier, Amsterdam
61. Papaefthymiou, V., Girerd, J.-J., Moura, I., and Münck, E. (1987) *J. Am. Chem. Soc.* **109,** 4703–4710
62. Zhou, J., Hu, Z., Münck, E., and Holm, R. H. (1996) *J. Am. Chem. Soc.* **118,** 1966–1980